

Supplementary Information - Magnetically responsive dry fluids<sup>†</sup>Filipa L. Sousa,<sup>\*a</sup> Rodney Bustamante,<sup>b</sup> Angel Millán,<sup>b</sup> Fernando Palacio,<sup>b</sup> Tito Trindade,<sup>a</sup> and Nuno J. O. Silva<sup>\*c</sup>

## 1 DLS

## 1.1 Methods

The hydrodynamic size ( $D_H$ ) distribution of the particles (beads) dispersed in the ferrofluids was determined by Dynamic Light Scattering (DLS) using the Zetasizer Nano ZS of Malvern (Fig. 1).

## 1.2 Description

DLS shows the existence of a monomodal distribution of NPs/beads. The relation between the average size of the NPs obtained by TEM and  $D_H$  suggests that FF- $\text{Fe}_3\text{O}_4$  is mainly composed of one  $\text{Fe}_3\text{O}_4$  NPs surrounded by a citrate shell of about 5 nm, while several  $\gamma\text{-Fe}_2\text{O}_3$  NPs can be present in the NP/polymer beads.

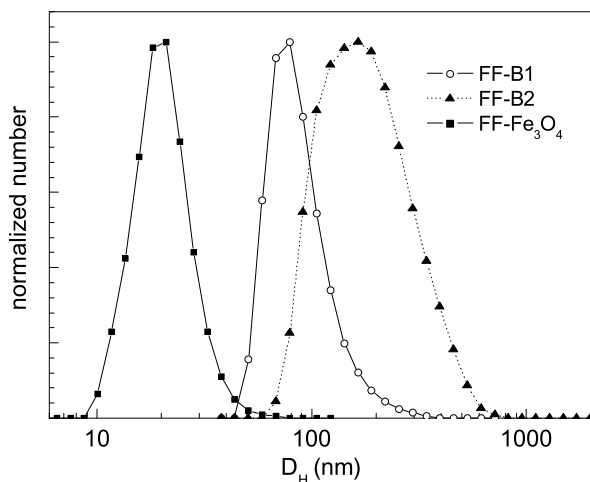


**Fig. 1** Distribution of the hydrodynamic diameters  $D_H$  obtained by DLS for the ferrofluids FF- $\text{Fe}_3\text{O}_4$ , FF-B1 and FF-B2.

<sup>a</sup> Departamento de Química and CICECO, Aveiro Institute of Nanotechnology, Universidade de Aveiro, 3810-193 Aveiro, Portugal. Fax: +351 234 370 084; Tel: +351 234 370 736; E-mail: filipalsousa@ua.pt

<sup>b</sup> Instituto de Ciencia de Materiales de Aragón, CSIC - Universidad de Zaragoza. Departamento de Física de la Materia Condensada, Facultad de Ciencias, 50009 Zaragoza, Spain.

<sup>c</sup> Departamento de Física and CICECO, Aveiro Institute of Nanotechnology Universidade de Aveiro, 3810-193 Aveiro, Portugal.

## 2 TEM

## 2.1 Methods

Transmission electron microscopy (TEM) was performed using a Jeol-2000 FXII microscope, with point-to-point and line-to-line resolutions of 0.28 nm and 0.14 nm, respectively. High Resolution TEM (HRTEM) was performed in a Tecnai G2-F30 Field Emission Gun microscope with a super-twin lens and 0.2 nm point-to-point resolution and 0.1 line resolution. Samples for TEM observations of the NPs dispersed in the ferrofluids were prepared by dip coating of lazy carbon coated copper grids.

## 2.2 Description

TEM shows the existence of a monomodal distribution of rounded NPs with size distribution typical of iron oxides obtained by precipitation methods and in accordance with that previously found<sup>1,2</sup>.

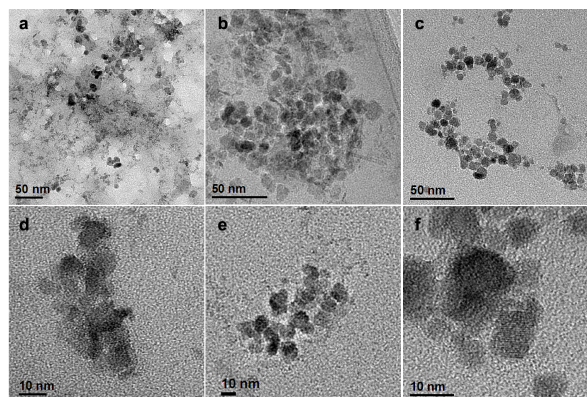


**Fig. 2** TEM images of the NPs dispersed in the ferrofluids. **a** and **d** correspond to FF-B1, **b** and **e** correspond to FF-B2 and **c** and **f** correspond to FF- $\text{Fe}_3\text{O}_4$ .

## 3 XRD

## 3.1 Methods

X-ray diffraction (XRD) measurements were performed at room temperature with a Philips X'Pert - MPD diffractome-

ter using monochromated CuK $\alpha$  radiation in the 30 - 80° 2 $\theta$  range at 0.04° resolution, and 4000 acquisition points per step. The incident beam optics included a Soller slit of 0.04 rad, a 10 mm fixed mask, a divergence fixed slit of 0.5° and an anti-scatter slit of 1°. The diffracted beam optics included a Soller slit of 0.04 rad and anti-scatter slit of 6.6 mm. The analysis of the diffraction patterns was performed by Rietveld refinement using the FullProf package<sup>3</sup>. The size effects were treated with the integral breadth method using the Voigt model for both the instrumental and intrinsic diffraction peak shape considering a Thompson-Cox-Hastings pseudo-Voigt convoluted with Axial divergence asymmetry function to describe the peak shape. The contribution of the instrument to the peaks broadening was determined by the refinement of the XRD pattern of a LaB<sub>6</sub> standard sample (NIST ref. 660a). The contribution of the finite size of the nanoparticles crystallites to the peaks broadening was taken into account by an isotropic model yielding an average apparent size.

### 3.2 Description

The XRD pattern of sample Fe<sub>3</sub>O<sub>4</sub>-powder shows the typical reflections of a spinel and can be fitted to the magnetite profile. Peak broadening is apparent due to finite-size effects. The average apparent size associated obtained by the refinement is close to the TEM average size, suggesting the high crystallinity of the NPs.

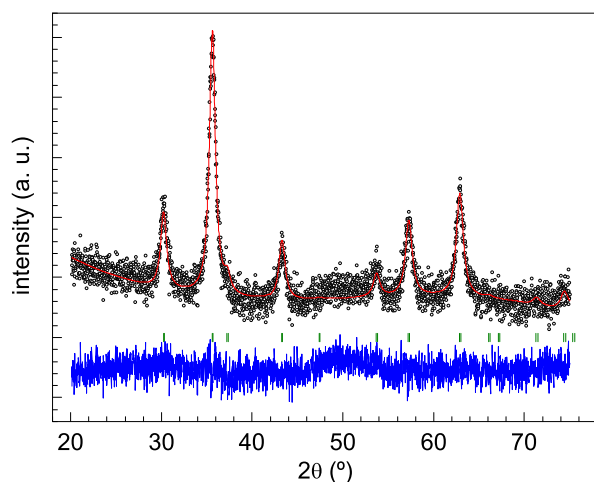


**Fig. 3** XRD pattern of sample Fe<sub>3</sub>O<sub>4</sub>-powder. Continuous (red) line corresponds to Rietveld refinement of a spinel (space group Fd $\bar{3}$ m) with cell parameter  $a = 8.359 \pm 1 \times 10^{-3}$  and an average apparent size of 7.9 nm ( $R_p=50.2\%$ ,  $R_{wp}=30.1\%$ ,  $R_{exp}=25.0\%$ ,  $\chi^2=1.45$ ). Vertical (green) lines represent the position of allowed Bragg peaks, while horizontal (blue) line represents the fit residues.

## 4 Contact Angle

### 4.1 Methods

Contact Angles were determined by the sessile drop method using a contact angle system OCA-20 (DataPhysics Instruments).

### 4.2 Description

Average contact angles of ferrofluids FF-Fe<sub>3</sub>O<sub>4</sub>, FF-B1 and FF-B2 on hydrophobic silica particles (Aerosil R812S) are 132, 129 and 135°, respectively, of the order of that previously found for water (108°),<sup>4</sup> confirming that the studied ferrofluids have a behavior similar to water when concerning wetting properties. We mention that surface roughness has a critical influence on the wetting properties of liquids on solids made of nanoparticles,<sup>4</sup> such that the differences observed between the ferrofluids here studied and water may be associated to differences in surface roughness.

## 5 NMR

### 5.1 Methods

The spectra Aerosil R812S were acquired on Bruker Avance III 400 spectrometer operating at a B<sub>0</sub> field of respectively 9.4 T. The <sup>1</sup>H and <sup>13</sup>C Larmor frequencies were 400.1, 100.6 MHz, respectively. All of the NMR experiments were performed at spinning rates in the range of 12 kHz.

### 5.2 Description

The <sup>1</sup>H spectra consist of two distinct resonances, the protons of the methyl groups appearing at  $\delta H \approx -0.58$  ppm, and the N-H protons around 3.5 ppm. While the <sup>13</sup>C CP MAS consist of a single resonance corresponding the carbon atoms of the methyl groups. This confirms the surface functionalization with C<sub>6</sub>H<sub>19</sub>NSi<sub>2</sub> groups, as indicated by the supplier.

## 6 Magnetic susceptibility

### 6.1 Methods and description

The magnetic susceptibility of sample Dry-B2 obtained in a restricted temperature range at  $f = 852$  Hz was repeated 8 months after the first measurement in order to check the stability of the susceptibility response. Figure 5 shows that the responses are identical, confirming the stability of the magnetic susceptibility response, within a period of at least 8 months.

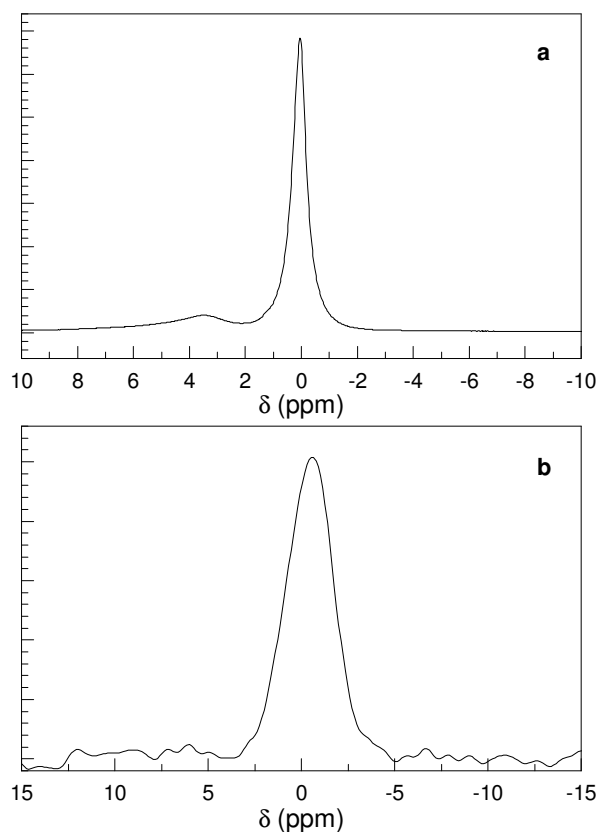


**Fig. 4** (a)  $^1\text{H}$  CP MAS NMR spectra and (b)  $^{13}\text{C}$  MAS NMR spectra of R182S.

## References

- 1 S. Nigam, K. Barick and D. Bahadur, *Journal of Magnetism and Magnetic Materials*, 2011, **323**, 237–243.
- 2 H. Amiri, R. Bustamante, A. Millán, N. J. O. Silva, R. Piñol, L. Gabilondo, F. Palacio, P. Arosio, M. Corti and A. Lascialfari, *Magn. Res. Med.*, 2011, **66**, 1715–1721.
- 3 J. Rodríguez-Carvajal, *Physica B*, 1993, **192**, 55.
- 4 L. Forny, K. Saleh, R. Denoyel and I. Pezron, *Langmuir*, 2010, **26**, 2333–2338.

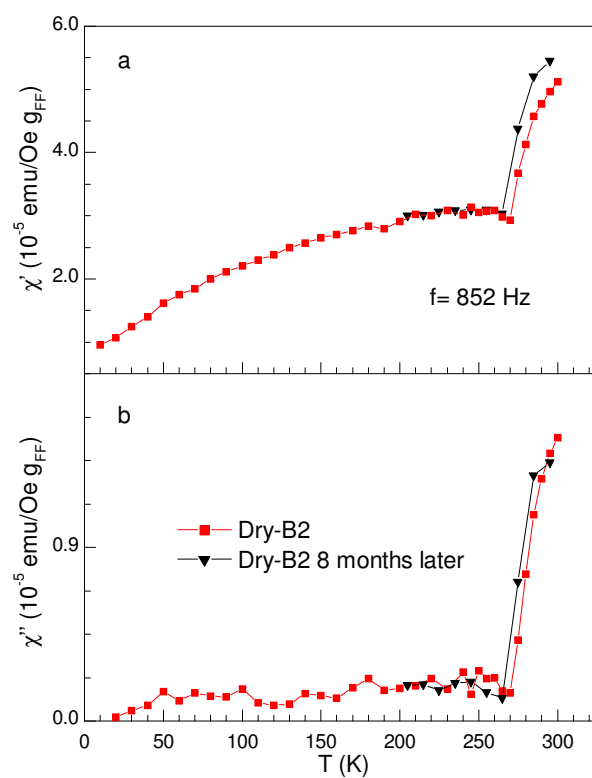


**Fig. 5** Temperature dependence of the in phase (a) and out of phase (b) magnetic susceptibility of sample Dry-B2 for  $f = 852$  Hz as shown in Fig. 4 of the manuscript and repeated eight months later in a restricted temperature range close to  $T_f$ .